Isogeometric Analysis, T-splines & Boundary-Element methods for Marine Hydrodynamics

P. Kaklis

University of Strathclyde & NTUA (National Technical University of Athens)

CAE Geometry Workshop – ITI - International TechneGroup
September 14-15, 2017, Cambridge (UK)

Outline

the wave resistance problem

the continuous problem

T-splines and isogeometric analysis

numerical results

output & recent work

the wave resistance (wr) problem – 1

consider the flow of a uniform stream of an ideal fluid with a free surface incident upon a surface-piercing or fully-submerged body. Decompose the velocity potential Φ in the form:

$$\Phi = -Ux + \varphi$$

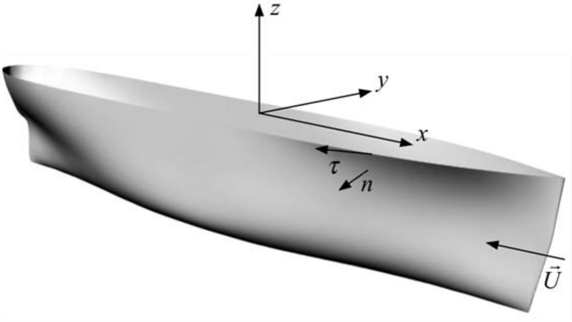

Figure 1: geometric configuration of the problem for a surface piercing body.

wr-problem: formulation – 2

the disturbance potential φ must satisfy:

- the Laplace equation

wr-problem: formulation – 2

the disturbance potential φ must satisfy:

- the Laplace equation
- body-boundary condition (of kinematic character)

wr-problem: formulation – 2

the disturbance potential φ must satisfy:

- the Laplace equation
- body-boundary condition (of kinematic character)
- a pair of conditions satisfied on the unknown free surface:
  - (i) kinematic condition: on the free surface the flow velocity must be tangential and
  - (ii) dynamic condition: the pressure on the free surface must be constant

wr-problem: formulation – 2

the disturbance potential φ must satisfy:

- the Laplace equation
- body-boundary condition (of kinematic character)
- a pair of conditions satisfied on the unknown free surface:
  - (i) kinematic condition: on the free surface the flow velocity must be tangential and
  - (ii) dynamic condition: the pressure on the free surface must be constant
- radiation condition ensuring existence and uniqueness: waves radiated by the body are directed mainly downwards

wr-problem: formulation – 2

the disturbance potential φ must satisfy:

- the Laplace equation
- body-boundary condition (of kinematic character)
- a pair of conditions satisfied on the unknown free surface:
  - (i) kinematic condition: on the free surface the flow velocity must be tangential and
  - (ii) dynamic condition: the pressure on the free surface must be constant
- radiation condition ensuring existence and uniqueness: waves radiated by the body are directed mainly downwards
- appealing to the theory of infinitesimal waves, the free-surface conditions are linearized by **neglecting higher-order terms with respect to** U and by applying the resulting equations on **the undisturbed free surface** instead of the unknown free surface

wr-problem: the Neumann-Kelvin problem – 3

the disturbance potential can be represented as:

$$\begin{aligned}\varphi(\mathbf{P}) \;=\; & \int_{\{wetted\ \ surface:\ S\}} \mu(\mathbf{Q}) G(\mathbf{P},\mathbf{Q}) dS(\mathbf{Q}) \;+ \\ & \frac{1}{k}\int_{\{waterline:\ \ell\}} \mu(\mathbf{Q}) G^*(\mathbf{P},\mathbf{Q}) n_1(\mathbf{Q}) \tau_2(\mathbf{Q}) d\ell(\mathbf{Q})\end{aligned}$$

where μ is the density of a single-layer distribution of the so-called Neumann-Kelvin singularities $G(\mathbf{P},\mathbf{Q})$:

$$4\pi G(\mathbf{P},\mathbf{Q}) = r^{-1} - (r')^{-1} + G^*(\mathbf{P},\mathbf{Q})$$

- $r = \|\mathbf{P}-\mathbf{Q}\|$, $r' = \|\mathbf{P}-\mathbf{Q}'\|$ with $\mathbf{Q}'$ denoting the image of $\mathbf{Q}$ with respect to the undisturbed free surface $z = 0$
- $G^*(\mathbf{P},\mathbf{Q})$ stands for the regular part, consisting of exponential decaying and wavelike components

wr-problem: Boundary Integral Equation (BIE) – 4

since $G(\mathbf{P},\mathbf{Q})$ satisfies

- the linearized condition on the undisturbed free surface and
- the conditions at infinity,

the Neumann-Kelvin problem is equivalently reformulated as a BIE on the body boundary S, characterized by a weakly singular kernel

$$\frac{\mu(\mathbf{P})}{2} - \int_S \mu(\mathbf{Q}) \frac{\partial G(\mathbf{P},\mathbf{Q})}{\partial n(\mathbf{P})} dS(\mathbf{Q})$$
$$\frac{1}{k}\int_\ell \mu(\mathbf{Q}) \frac{\partial G^*(\mathbf{P},\mathbf{Q})}{\partial n(\mathbf{P})} n_1(\mathbf{Q})\tau_2(\mathbf{Q}) d\ell(\mathbf{Q}) = \mathbf{U}\cdot\mathbf{n}(\mathbf{P}), \quad \mathbf{P},\mathbf{Q} \in S.$$

$k = g/U^2$ is the characteristic wavenumber, controlling the wavelength of the transverse ship waves

wr-problem: T-splines – 5

- the basic object underlying T-spline technology [1], [2] is the T-mesh

[1] Sederberg, T. W., Zheng, J. and Song, X., 2003 **Knot intervals and multi-degree splines**, *Computer Aided Geometric Design*, vol. 20, 455-468

[2] Sederberg, T. W., Zheng, J., Bakenov, A. and Nasri, A (2003) **T-splines and TNURCCs**, *ACM Transactions on Graphics* , vol. 22, 477-484.

wr-problem: T-splines – 5

- the basic object underlying T-spline technology [1], [2] is the T-mesh
- surfaces: a T-mesh is a polygonal mesh

[1] Sederberg, T. W., Zheng, J. and Song, X., 2003 **Knot intervals and multi-degree splines**, *Computer Aided Geometric Design*, vol. 20, 455-468

[2] Sederberg, T. W., Zheng, J., Bakenov, A. and Nasri, A (2003) **T-splines and TNURCCs**, *ACM Transactions on Graphics* , vol. 22, 477-484.

wr-problem: T-splines – 5

- the basic object underlying T-spline technology [1], [2] is the T-mesh
- surfaces: a T-mesh is a polygonal mesh
- each element is a quadrilateral whose edges are permitted to contain T-junctions

[1] Sederberg, T. W., Zheng, J. and Song, X., 2003 **Knot intervals and multi-degree splines**, *Computer Aided Geometric Design*, vol. 20, 455-468

[2] Sederberg, T. W., Zheng, J., Bakenov, A. and Nasri, A (2003) **T-splines and TNURCCs**, *ACM Transactions on Graphics* , vol. 22, 477-484.

wr-problem: T-splines – 5

- the basic object underlying T-spline technology [1] , [2] is the T-mesh
- surfaces: a T-mesh is a polygonal mesh
- each element is a quadrilateral whose edges are permitted to contain T-junctions
- a control point, $\mathbf{P}_A \in \mathbb{R}^3$ and a control weight, $w_A \in \mathbb{R}^+$, where the index A denotes a global control point number, is assigned to every vertex in the T-mesh

---

[1] Sederberg, T. W., Zheng, J. and Song, X., 2003 **Knot intervals and multi-degree splines**, *Computer Aided Geometric Design*, vol. 20, 455-468

[2] Sederberg, T. W., Zheng, J., Bakenov, A. and Nasri, A (2003) **T-splines and TNURCCs**, *ACM Transactions on Graphics* , vol. 22, 477-484.

wr-problem: T-splines – 5

- the basic object underlying T-spline technology [1] , [2] is the T-mesh
- surfaces: a T-mesh is a polygonal mesh
- each element is a quadrilateral whose edges are permitted to contain T-junctions
- a control point, $\mathbf{P}_A \in \mathbb{R}^3$ and a control weight, $w_A \in \mathbb{R}^+$, where the index A denotes a global control point number, is assigned to every vertex in the T-mesh
- an extraordinary point is an interior vertex that is not a T-junction and whose valence $\neq 4$.

---

[1] Sederberg, T. W., Zheng, J. and Song, X., 2003 **Knot intervals and multi-degree splines**, *Computer Aided Geometric Design*, vol. 20, 455-468

[2] Sederberg, T. W., Zheng, J., Bakenov, A. and Nasri, A (2003) **T-splines and TNURCCs**, *ACM Transactions on Graphics* , vol. 22, 477-484.

wr-problem: T-splines – 6

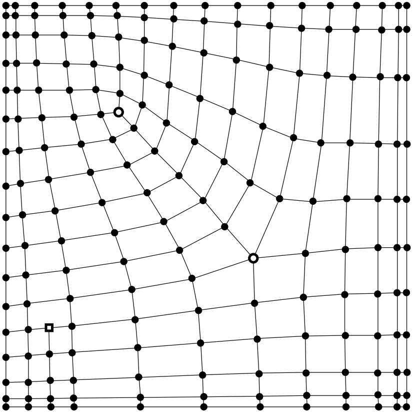

Figure 2: an unstructured T-mesh: the single T-junction is denoted by a hollow square – the two extraordinary points are denoted by hollow circles

wr-problem: T-spline based isogeometric BEM – 7

a T-spline basis for our geometry

we assume that the body-boundary is **accurately** represented as a T-spline surface:

$$S = \bigcup_{e=1}^{n_e} S_e, \quad S_e(\tilde{\boldsymbol{\xi}}) = \sum_{i=1}^{n_{cp}} \mathbf{d}_i R_i^e(\tilde{\boldsymbol{\xi}}), \quad \tilde{\boldsymbol{\xi}} \in \tilde{\Omega}_e,$$

where

- n_{cp} is the number of control points or T-mesh vertices $\mathbf{d}_i$ in the T-mesh

wr-problem: T-spline based isogeometric BEM – 7

a T-spline basis for our geometry

we assume that the body-boundary is **accurately** represented as a T-spline surface:

$$S = \bigcup_{e=1}^{n_e} S_e, \quad S_e(\tilde{\xi}) = \sum_{i=1}^{n_{cp}} \mathbf{d}_i R_i^e(\tilde{\xi}), \quad \tilde{\xi} \in \tilde{\Omega}_e,$$

where

- n_{cp} is the number of control points or T-mesh vertices $\mathbf{d}_i$ in the T-mesh
- R_i^e is the restriction of the rational T-spline basis function R_i at $\tilde{\Omega}_e$

wr-problem: T-spline based isogeometric BEM – 7

a T-spline basis for our geometry

we assume that the body-boundary is **accurately** represented as a T-spline surface:

$$S = \bigcup_{e=1}^{n_e} S_e, \quad S_e(\tilde{\xi}) = \sum_{i=1}^{n_{cp}} \mathbf{d}_i R_i^e(\tilde{\xi}), \quad \tilde{\xi} \in \tilde{\Omega}_e,$$

where

- n_{cp} is the number of control points or T-mesh vertices $\mathbf{d}_i$ in the T-mesh
- R_i^e is the restriction of the rational T-spline basis function R_i at $\tilde{\Omega}_e$
- n_e is the number of elements

wr-problem: T-spline- & IGA- based BEM – 8

the isogeometric (IGA) concept

the unknown source-sink surface distribution μ is **approximated** by the very same T-splines basis used for the body-boundary representation, that is:

$$\mu(\mathbf{P}) = \sum_{i=1}^{n_{cp}} \mu_i \tilde{R}_i(\mathbf{P}), \quad \mathbf{P} \in S,$$

where $\tilde{R}_i(\mathbf{P}) \equiv R_i^e(\tilde{\boldsymbol{\xi}}(\mathbf{P})), \mathbf{P} \in S_e$

wr-problem: T-spline- & IGA- based BEI – 9

T-spline based IGA-BEM

inserting the T-spline approximation of μ into the BIE, we get:

$$\frac{1}{2}\sum_{i=1}^{n_{cp}} \mu_i \tilde{R}_i(\mathbf{P}) - \sum_{i=1}^{n_{cp}} \mu_i \mathbf{n}(\mathbf{P}) \cdot \mathbf{u}_i(\mathbf{P}) = \mathbf{U} \cdot \mathbf{n}(\mathbf{P}), \quad \mathbf{P} \in S,$$

where

$$\begin{aligned} \mathbf{u}_i(\mathbf{P}) \;\; = \;\; & \int_S \tilde{R}_i(\mathbf{Q}) \nabla_P G(\mathbf{P}, \mathbf{Q}) dS(\mathbf{Q}) + \\ & + k^{-1} \int_\ell \tilde{R}_i(\mathbf{Q}) \nabla_P G^*(\mathbf{P}, \mathbf{Q}) n_1(\mathbf{Q}) \tau_2(\mathbf{Q}) d\ell(\mathbf{Q}) \end{aligned}$$

are the so-called induced velocity factors

- next we collocate the BIE by specifying n_{cp} collocation points $\mathbf{P}_j, j = 1, \ldots, n_{cp}$, on S

wr-problem: T-spline- & IGA- based BEI collocated – 10

- next we collocate the BIE by specifying n_{cp} collocation points $\mathbf{P}_j, j = 1, \ldots, n_{cp}$, on S
- for smooth ship hulls, these points are choosen to be the *1-ring collocation points* [3] for both the non-extraordinary and extraordinary vertices of the T-mesh

[3] M. A. Scott, R. N. Simpson, J. A. Evans, S. Lipton, S. P. A. Bordas, T. J. R. Hughes and T.W. Sederberg (2013) **Isogeometric boundary element analysis using unstructured T-splines**, *Computer Methods in Applied Mechanics and Engineering*, vol. 254, 197-221.

wr-problem: T-spline- & IGA- based BEI collocated – 10

- next we collocate the BIE by specifying n_{cp} collocation points $\mathbf{P}_j, j = 1, \ldots, n_{cp}$, on S
- for smooth ship hulls, these points are choosen to be the *1-ring collocation points* [3] for both the non-extraordinary and extraordinary vertices of the T-mesh
- this definition of collocation points is a generalization of the Greville abscissae for the cases of unstructured grids, T-junctions and extraordinary points

[3] M. A. Scott, R. N. Simpson, J. A. Evans, S. Lipton, S. P. A. Bordas, T. J. R. Hughes and T.W. Sederberg (2013) **Isogeometric boundary element analysis using unstructured T-splines**, *Computer Methods in Applied Mechanics and Engineering*, vol. 254, 197-221.

wr-problem: T-spline- & IGA- based BEI collocated – 10

- next we collocate the BIE by specifying n_{cp} collocation points $\mathbf{P}_j, j = 1, \ldots, n_{cp}$, on S
- for smooth ship hulls, these points are choosen to be the *1-ring collocation points* [3] for both the non-extraordinary and extraordinary vertices of the T-mesh
- this definition of collocation points is a generalization of the Greville abscissae for the cases of unstructured grids, T-junctions and extraordinary points

we thus obtain the following linear system of equations with respect to the unknown coefficients μ_i:

$$\sum_{i=1}^{n_{cp}} \mu_i \left[\tilde{R}_i(\mathbf{P}_j) - 2\mathbf{n}(\mathbf{P}_j) \cdot \mathbf{u}_i(\mathbf{P}_j) \right] = 2\mathbf{U} \cdot \mathbf{n}(\mathbf{P}_j),\ j = 1, \ldots, n_{cp}.$$

[3] M. A. Scott, R. N. Simpson, J. A. Evans, S. Lipton, S. P. A. Bordas, T. J. R. Hughes and T.W. Sederberg (2013) **Isogeometric boundary element analysis using unstructured T-splines**, *Computer Methods in Applied Mechanics and Engineering*, vol. 254, 197-221.

- in the final linear sysyem, the integrals involved in the calculation of the induced velocity factors are localized to integrals over Bézier elements using the Bézier extraction framework described in S

- in the final linear sysyem, the integrals involved in the calculation of the induced velocity factors are localized to integrals over Bézier elements using the Bézier extraction framework described in S
- since these singular integrals are defined in the Cauchy Principal Value (CPV) sense, we employ the following technique:

wr-problem: T-spline- & IGA- based BEI collocated – 11

- in the final linear sysyem, the integrals involved in the calculation of the induced velocity factors are localized to integrals over Bézier elements using the Bézier extraction framework described in S
- since these singular integrals are defined in the Cauchy Principal Value (CPV) sense, we employ the following technique:
- we exclude an $\epsilon-$neighborhood, with $\epsilon \to 0$, around the singularity at the collocation point $\mathbf{P_j}$

- in the final linear sysyem, the integrals involved in the calculation of the induced velocity factors are localized to integrals over Bézier elements using the Bézier extraction framework described in *S*
- since these singular integrals are defined in the Cauchy Principal Value (CPV) sense, we employ the following technique:
- we exclude an $\epsilon-$neighborhood, with $\epsilon \to 0$, around the singularity at the collocation point $\mathbf{P_j}$
- in order to maintain a uniform numerical scheme for the calculation of the CPV integrals, we need to make sure that the collocation point $\mathbf{P_j}$ lies in the interior of Bézier elements

- in the final linear sysyem, the integrals involved in the calculation of the induced velocity factors are localized to integrals over Bézier elements using the Bézier extraction framework described in S
- since these singular integrals are defined in the Cauchy Principal Value (CPV) sense, we employ the following technique:
- we exclude an $\epsilon-$neighborhood, with $\epsilon \to 0$, around the singularity at the collocation point $\mathbf{P_j}$
- in order to maintain a uniform numerical scheme for the calculation of the CPV integrals, we need to make sure that the collocation point $\mathbf{P_j}$ lies in the interior of Bézier elements
- if this is not the case, we shift appropriately the corresponding collocation point

wr: tests: prolate spheroid in infinite domain - 12

velocity error distribution for T-spline refinement

an analytical expression of the velocity on the surface of the spheroid is available

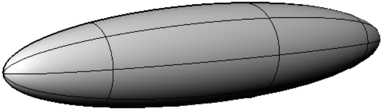

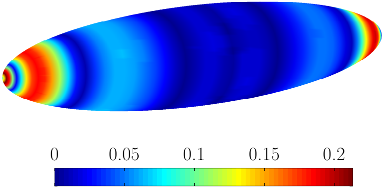

Figure 3: DoF = 81

wr: tests: prolate spheroid in infinite domain - 12

velocity error distribution for T-spline refinement

an analytical expression of the velocity on the surface of the spheroid is available

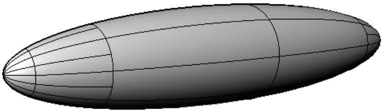

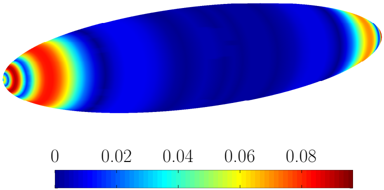

Figure 3: DoF = 131

velocity error distribution for T-spline refinement

an analytical expression of the velocity on the surface of the spheroid is available

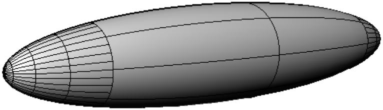

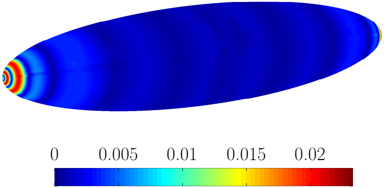

Figure 3: DoF = 279

wr: tests: prolate spheroid in infinite domain - 12

velocity error distribution for T-spline refinement

an analytical expression of the velocity on the surface of the spheroid is available

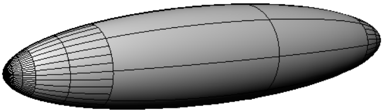

Figure 3: DoF = 555

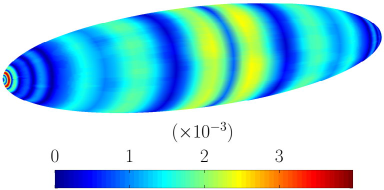

wr: tests: prolate spheroid in infinite domain - 12

velocity error distribution for T-spline refinement

an analytical expression of the velocity on the surface of the spheroid is available

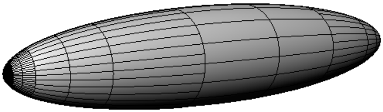

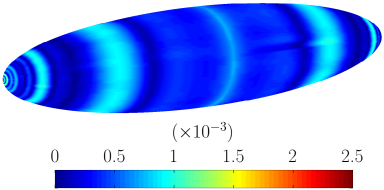

Figure 3: DoF = 875

velocity-error for NURBS refinement

an analytical expression of the velocity on the surface of the spheroid is available

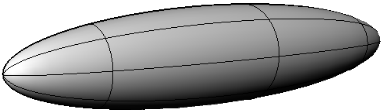

Figure 4: DoF = 81

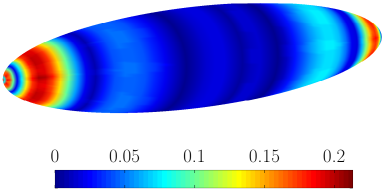

wr: tests: prolate spheroid in infinite domain - 13

velocity-error for NURBS refinement

an analytical expression of the velocity on the surface of the spheroid is available

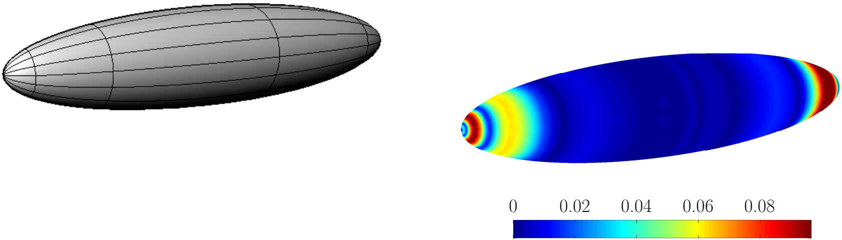

Figure 4: DoF = 143

wr: tests: prolate spheroid in infinite domain - 13

velocity-error for NURBS refinement

an analytical expression of the velocity on the surface of the spheroid is available

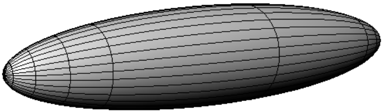

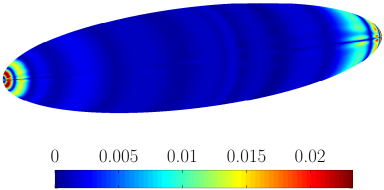

Figure 4: DoF = 315

velocity-error for NURBS refinement

an analytical expression of the velocity on the surface of the spheroid is available

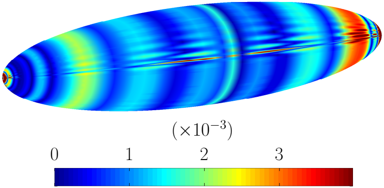

Figure 4: DoF = 703

velocity-error for NURBS refinement

an analytical expression of the velocity on the surface of the spheroid is available

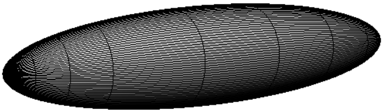

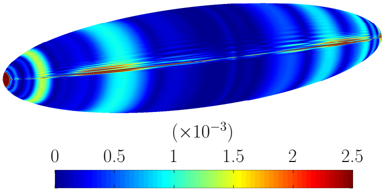

Figure 4: DoF = 1587

wr: tests: prolate spheroid infinite domain - 14

L^2-error convergence: T-splines vs NURBS

- T-spline meshes are locally h-refined based on comparison with the analytic solution
- NURBS results correspond to the unique NURBS refinement of each of the T-spline meshes

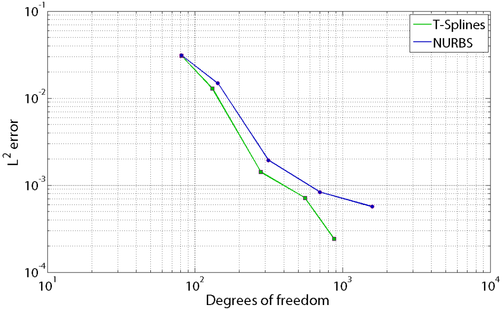

modeling via Rhinoceros T-spline plugin

- the T-spline hull is locally of polynomial degree three in both directions with 79 control points

wr: tests: surface piercing ship-hull – 15

modeling via Rhinoceros T-spline plugin

- the T-spline hull is locally of polynomial degree three in both directions with 79 control points
- since no extraordinary control points exist, a unique conversion of the T-spline rep into a single NURBS patch is feasible with 132 control points

wr: tests: surface piercing ship-hull – 15

modeling via Rhinoceros T-spline plugin

- the T-spline hull is locally of polynomial degree three in both directions with 79 control points
- since no extraordinary control points exist, a unique conversion of the T-spline rep into a single NURBS patch is feasible with 132 control points

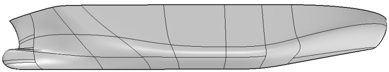

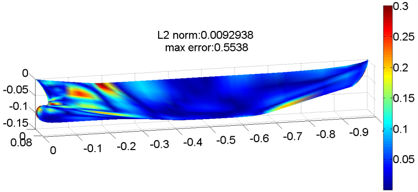

Figure 5: DoF = 79

modeling via Rhinoceros T-spline plugin

- the T-spline hull is locally of polynomial degree three in both directions with 79 control points
- since no extraordinary control points exist, a unique conversion of the T-spline rep into a single NURBS patch is feasible with 132 control points

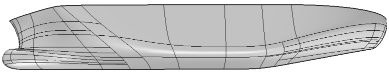

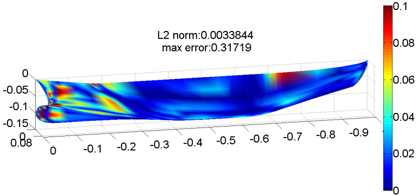

Figure 5: DoF = 160

wr: tests: surface piercing ship-hull – 15

modeling via Rhinoceros T-spline plugin

- the T-spline hull is locally of polynomial degree three in both directions with 79 control points
- since no extraordinary control points exist, a unique conversion of the T-spline rep into a single NURBS patch is feasible with 132 control points

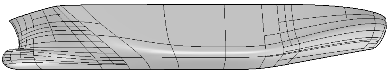

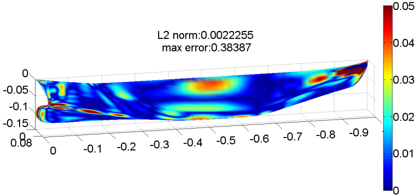

Figure 5: DoF = 242

wr: tests: surface piercing ship-hull – 15

modeling via Rhinoceros T-spline plugin

- the T-spline hull is locally of polynomial degree three in both directions with 79 control points
- since no extraordinary control points exist, a unique conversion of the T-spline rep into a single NURBS patch is feasible with 132 control points

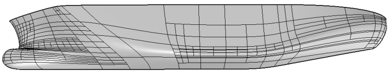

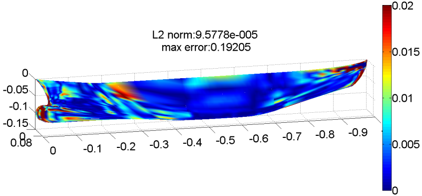

Figure 5: DoF = 519

wr: tests: surface piercing ship-hull – 16

L^2-error convergence: T-splines vs NURBS

we have constructed a “reference solution” of the problem by inserting uniformly 9 knots in every knot interval of the original NURBS representation and computed the IGA-BEM approximation of μ for the resulting NURBS surface.

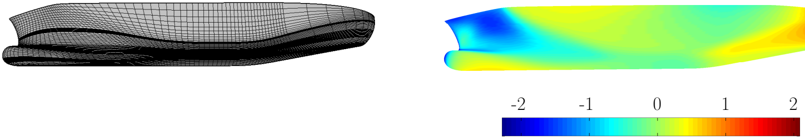

Figure 6: uniformly refined NURBS mesh (left) and corresponding reference solution (right)

L^2-error convergence: T-splines vs NURBS

we have constructed a “reference solution” of the problem by inserting uniformly 9 knots in every knot interval of the original NURBS representation and computed the IGA-BEM approximation of μ for the resulting NURBS surface.

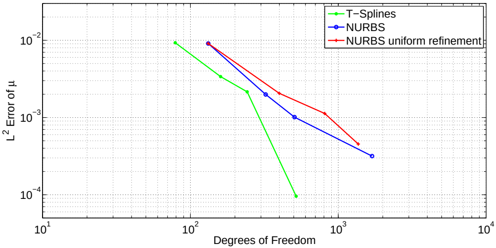

Figure 6: T-spline based local refinement process, the corresponding NURBS refinement and the refinement process resulting from inserting uniformly r knots in each parametric interval of the original NURBS representation

◇ **Analysis** (IGA-BEM, NURBS, T-splines - 2D potential flows, wave resistance, 3D flows with lift)

- S.P. Chouliaras, P.D. Kaklis, A.-A.I. Ginnis, K.V. Kostas and C.G. Politis, **"An IGA-BEM Method for the Open-Water Marine Propeller Flow Problem"**, *International Conference on Isogeometric Analysis, IGA-2017*, 11-13 September 2017, Pavia (IT).

- A.-A.I. Ginnis, K.V. Kostas, C.G. Politis, P.D. Kaklis, K.A. Belibassakis, T.P. Gerostathis, M.A. Scott and T.J.R. Hughes, **"Isogeometric Boundary- Element Analysis for the Wave-Resistance Problem using T-splines"**, *Computer Methods in Applied Mechanics and Engineering*, **279**, 425-439, (2014).

- K.A. Belibassakis, Th.P. Gerosthathis, K.V. Kostas, C.G. Politis, P.D. Kaklis, A.I. Ginnis and C. Feurer, **"A BEM-Isogeometric method for the ship wave-resistance problem"**, *Ocean Engineering*, **60**, 53-67, (2013).

- C. G. Politis, A. I. Ginnis, P. D. Kaklis, K. A. Belibassakis and C. Feurer, **"An Isogeometric BEM for Exterior Potential-flow Problems in the Plane"**, in *Proceedings of the SIAM/ACM Joint Conference on Geometric and Physical Modeling*, October 5-8, 2009, San Francisco, California, USA, art. no. 1629302, pp. 349-354.

output & recent work – 18

◇ **shape optimization** (IGA-BEM, T-spline based parametric modelers - wave resistance, 2D flows with lift, boundary-layer corrections)

• Kostas, K.V., Ginnis, A.I., Politis, C.G., Kaklis, P.D, **"Shape-optimization of 2D hydrofoils using an Isogeometric BEM solver"**, *Computer Aided Design*, **82**, 79-87, (2017).

• Kostas, K.V., Ginnis, A.I., Politis, C.G., Kaklis, P.D, **"Shape-optimization of 2D hydrofoils using one-way coupling of an IGA-BEM solver with a boundary-layer model"**, *Coupled Problems 2017 – VII International Conference on Coupled Problems in Science and Engineering*, June 12-14, 2017, Rhodes (GR).

• K.V. Kostas, A.-A.I. Ginnis, C.G. Politis and P.D. Kaklis, **"Ship-Hull Shape Optimization with a T-spline based BEM-Isogeometric Solver"**, *Computer Methods in Applied Mechanics and Engineering*, **284**, 611-622, (2015).

funding context

- **EXCITING**: Exact Geometry Simulation for Optimized Design of Vehicles and Vessels, Framework Programme: FP7-CP-FP, 2008-12.
- **THALIS**: European Social Fund – the Operational Program on Education and Lifelong Learning.
- **ARCADES**: Algebraic Representations for Computer-Aided Design of Complex Shapes, Horizon 2020, Marie Slodowska Curie - Innovative Training Networks Action, 2016-19.
- **AROMATH**: Algebraic Geometric Modeling and Algorithms, Équipe Projet INRIA Commune Européenne, 2016-20.

THANK YOU!